

## Strength of thermal undulations of phospholipid membranes

V. I. Gordeliy,<sup>1,2,3,\*</sup> V. Cherezov,<sup>3,4</sup> and J. Teixeira<sup>5</sup>

<sup>1</sup>*IBI-2: Institute for Structural Biology, Research Center Juelich, D-52425 Juelich, Germany*

<sup>2</sup>*Center for Biophysics and Physical Chemistry of Supramolecular Structures, Moscow Institute for Physics and Technology, Dolgoprudny, Russia*

<sup>3</sup>*Frank Laboratory of Neutron Physics, Joint Institute for Nuclear Research, 141980 Dubna, Russia*

<sup>4</sup>*Chemistry Department, The Ohio State University, Columbus, Ohio 43210, USA*

<sup>5</sup>*Laboratoire Léon Brillouin (CEA-CNRS), CE Saclay, 91191 Gif-sur-Yvette Cedex, France*

(Received 25 July 2005; published 20 December 2005)

The temperature dependence of intermembrane interactions in freely suspended multilamellar membranes of dimiristoylphosphatidylcholine in D<sub>2</sub>O was studied using small-angle neutron scattering (SANS) and high-resolution x-ray diffraction (HRXRD). The study reveals that the Helfrich's undulation force is the dominating repulsion force at temperatures above 48.6 °C and intermembrane distances larger than 20.5 Å. At ~77 °C the onset of the unbinding transition in the multilamellar membranes is observed. This transition has a continuous behavior in agreement with theoretical predictions and proceeds in accordance with a two-state model. Complementary analysis of SANS and HRXRD data permits accurate calculation of the fundamental undulation force constant  $c_{fl}$ . The obtained value of  $c_{fl}=0.111\pm 0.005$  is in good agreement with theoretical calculations. The results of this work demonstrate a key role of Helfrich's undulations in the balance of intermembrane interactions of lipid membranes under physiological temperatures and suggest that thermal undulations play an important part in the interactions of biological membranes. The agreement of the predictions with the experimental data confirms that lipid membranes can be considered as random fluctuating surfaces that can be described well by current theoretical models and that they can serve as a powerful tool for studying behavior of such surfaces.

DOI: [10.1103/PhysRevE.72.061913](https://doi.org/10.1103/PhysRevE.72.061913)

PACS number(s): 87.15.Kg, 87.16.Dg, 87.64.Bx, 61.30.Cz

### I. INTRODUCTION

Lipid bilayers are the main structural elements of biological membranes [1] and are widely used to mimic their properties [2]. Closed lipid membranes, or liposomes, have important practical applications, for instance, in drug delivery [3]. Membranes are also of great interest for the statistical physics of fluctuating (random) surfaces [4–6]. Fluctuating surfaces include a wide range of physical objects from biomembranes to world sheets swept out in time by strings between elementary particles in the theory of fundamental interactions [7–9]. Studying intermembrane interactions is particularly important because of their relevance to biomembrane fusion [2–10]. However, in spite of considerable recent progress in this area, several fundamental problems remain to be solved.

This paper is concerned with the problem of unbinding transitions in multilamellar membranes, and the related question of the magnitude of the undulation force contribution to the balance of intermembrane interactions. The existing disagreement between theoretical calculations and experimentally determined values of the universal constant  $c_{fl}$  of the undulation force acting between thermally fluctuating multilamellar membranes is so significant that it casts serious doubts on the validity of the currently held theoretical models of biological and lipid membranes.

In this paper we begin by introducing the forces acting between electrically neutral lipid membranes and describe

their thermal dependence. Next, a relationship between the balance of these forces and the unbinding phenomenon is presented, following which a conflict between the theoretical treatment and the experimental results of the unbinding transition and on the value of  $c_{fl}$  is discussed. Finally, an approach to the investigation of intermembrane interactions via the complementary use of small-angle neutron scattering (SANS) and high resolution x-ray diffraction (HRXRD) is presented and results are discussed.

### II. THEORY

The current view of the balance of forces acting between uncharged membranes indicates the presence of three main contributions: a strong short-range repulsion (often called the “hydration” force), long-range van der Waals attraction, and long-range Helfrich's undulation repulsion [4,10–14].

#### A. Short-range repulsion (“hydration”) force

It is well established experimentally that the energy per unit volume of the short-range repulsion between two adjacent membranes varies exponentially with the intermembrane distance  $d_w$ :

$$f_H(d_w) = A_H \exp(-d_w/\lambda), \quad (1)$$

where  $A_H \approx 10^{-17} - 10^{-18}$  J/m<sup>2</sup> and  $\lambda \approx 0.1 - 0.24$  nm for phospholipid membranes [11,12,15]. The origin of this force is still under investigation [11–18]. One of the hypotheses attributes this force to the intrinsic structure of the lipid-

\*Corresponding author.

water interface, meaning that the propagation of the interaction (the hydration force) is determined by the water properties [11,12,15]. The hydration force is expected to weaken as temperature increases. An alternative point of view attributes the short-range repulsion force to the out-of-plane thermal fluctuations (protrusions) of lipid molecules [13,14,16–18]. Such an entropic force, on the other hand, should increase with temperature. Indeed, the decay length of the force  $\lambda$  is proportional to the temperature ( $\lambda \sim T/\gamma$ ), where  $\gamma$  is the interfacial energy [13,14]. In addition, the interfacial energy should decrease upon heating [19]. Renormalization of the short-range repulsion, assuming simultaneous presence of both origins of the forces, yields comparable values and has been attempted as well [20–22]. In this case the net force increases with temperature, and this behavior results from the temperature dependent entropic force due to the protrusions [21,22].

### B. Long-range van der Waals attraction

The van der Waals attraction between two membranes of thickness  $d_b$  resulting from different polarizabilities of the lipid and water molecules is given by [11,23]

$$f_{vdW} = -\frac{H}{12\pi} \left[ \frac{1}{d_w^2} - \frac{2}{(d_w + d_b)^2} + \frac{1}{(d_w + 2d_b)^2} \right], \quad (2)$$

where  $H \approx 10^{-21} - 10^{-20}$  J is the Hamaker constant [23–25]. There is no good agreement between different estimations of the Hamaker constant for lipid bilayers. For instance, measurements of forces between dimiristoylphosphatidylcholine (DMPC) membranes with surface force apparatus resulted in values of  $H = (7.5 \pm 1) \times 10^{-21}$  J [24] and  $H = (1.3 \pm 0.2) \times 10^{-21}$  J [25].

The van der Waals repulsion exhibits different regimes of power law decay depending on the intermembrane distance. At small intermembrane distances ( $d_w \ll d_b$ ),  $f_{vdW} \propto 1/d_w^2$ ; at larger  $d_w$  ( $d_b \ll d_w$ ),  $f_{vdW} \propto 1/d_w^4$ ; and finally, at sufficiently large  $d_w$  the retardation effects lead to  $f_{vdW} \propto 1/d_w^5$  [23]. The Hamaker constant is temperature dependent [23],

$$H = \frac{3k_B T}{4} \left( \frac{\epsilon_l - \epsilon_w}{\epsilon_l + \epsilon_w} \right)^2 + \frac{3h\nu_e}{16\sqrt{2}} \frac{(n_l^2 - n_w^2)^2}{(n_l^2 + n_w^2)^{3/2}}, \quad (3)$$

where  $k_B$  is the Boltzmann's constant;  $\epsilon_l$  and  $\epsilon_w$  are the static dielectric constants of lipids and water, respectively;  $n_l$  and  $n_w$  are the refractive indices; and  $\nu_e$  is the ultraviolet frequency. Note that the Hamaker constant in its explicit form, Eq. (3), depends linearly on the temperature.

### C. Long-range undulation repulsion

The third contribution to the balance of intermembrane forces comes from thermally excited membrane undulations as was suggested by Helfrich [4]. This entropic interaction follows a long-range power law:

$$f_{und} = c_{fl} \frac{(k_B T)^2}{k d_w^2}, \quad (4)$$

where  $k$  is the membrane rigidity and  $c_{fl}$  is the universal fluctuation constant. This equation was derived under the

assumption that membranes do not interact with each other through any other forces except for the hard-wall confinement.

As it follows from Eq. (4) the  $f_{und}$  is proportional to the square of the temperature. However, one can expect an even stronger thermal dependence of the undulation force. Indeed, the bending rigidity  $k$  is approximately proportional to the square of the length of the hydrocarbon chains [26]. It was shown recently [17] and confirmed in the present work that the lipid bilayer shrinks when temperature increases. In addition, it is predicted that the bending elasticity must be renormalized in order to take protrusions into account [21]. As a consequence,  $k$  is additionally reduced when temperature increases.

It is worth noting that the experimentally determined values of  $k$  range from  $\sim 10^{-20}$  to  $10^{-19}$  J for phospholipid membranes. For example, reported values of the bending rigidity of DMPC vesicles are very scattered:  $(1.15 \pm 0.15) \times 10^{-19}$  J [27],  $(0.35 - 0.65) \times 10^{-19}$  J [28],  $(0.56 \pm 0.06) \times 10^{-19}$  J [29], and  $1.8 \times 10^{-19}$  J [30].

### D. Value of the undulation force constant $c_{fl}$

The universal constant  $c_{fl}$  [see Eq. (4)] is a measure of the strength of fluctuations and plays an important role in the statistical physics of self-avoiding surfaces with extrinsic curvature stiffness [7,8]. The initial estimate  $c_{fl} = 3\pi^2/128 \approx 0.23$  was made by Helfrich [4] using de Gennes continuum harmonic approximation for the elastic energy per unit volume,

$$f = \frac{1}{2} B \left( \frac{\partial u}{\partial z} \right)^2 + \frac{1}{2} K \left( \frac{\partial^2 u}{\partial x^2} + \frac{\partial^2 u}{\partial y^2} \right)^2, \quad (5)$$

[where  $u = u(x, y, z)$  is the locally varying displacement of the bilayers in normal to the membrane direction;  $B$  is the compressibility modulus and  $K$  is the bending modulus of the stack of the membranes] applied to a pure hard-wall case [4]. However, further more sophisticated calculations gave values of  $c_{fl}$  about two times smaller than  $3\pi^2/128$  [9,31–38]. For example, renormalization group treatment of the entropic interaction in lamellar phases yields  $c_{fl} \sim 0.081$  [33]. Monte Carlo estimations give  $0.101 \pm 0.002$  [35],  $0.106$  [36], recent analytical calculation of the constant yields the value  $0.099$  for a single membrane [39], and the most recent calculations for a multilamellar stack of membranes give  $c_{fl} = 0.115 \pm 0.005$  [40],  $0.111 \pm 0.006$  [38],  $0.113 \pm 0.005$  [41]. All these values coincide well, and all of them are smaller than the first estimate [4] roughly by a factor of 2. On the other hand, results of the high-resolution x-ray experiments [42–44] agree surprisingly well with the first estimate of  $c_{fl} = 3\pi^2/128$  by Helfrich. Understanding the origin of this discrepancy is of great importance [9,31–38,45]. Indeed, if the discrepancy between theory and experiment cannot be resolved then the basis of the physical model of membranes (for instance, applicability of harmonic approximation) must be revised. Accordingly, a significant part of this work is devoted to accurate estimation of the value of  $c_{fl}$ .

### E. Membrane unbinding

The superposition of the three energies described above,

$$f(d_w) = f_H(d_w) + f_{vdW}(d_w) + f_{und}(d_w), \quad (6)$$

shows that at low temperatures  $f(d_w)$  has a global minimum at a small finite  $d_w$ , which corresponds to the bound state of the membrane. However, at higher temperatures this minimum shifts to an infinite distance between membranes (i.e., to the unbound state of the membrane). At a certain intermediate temperature  $T_c$ , the bound and unbound states have the same free energy. Thus membranes would exhibit a discontinuous (first order) transition from bound to unbound state in accordance with the superposition model [45,46]. However, it has been shown that the superposition fails if  $f(d_w)$  has an attractive part which decays faster than  $1/d_w^2$  at large  $d_w$  [40,45]. This is exactly what happens in the case of interacting phospholipid membranes due to the decay of the van der Waals forces. Renormalization group treatment of the competition between short-range repulsive, attractive van der Waals, and steric (due to undulations) contributions results in the prediction of a qualitatively different character of the unbinding transition [45]. Within this context, a continuous (second order) transition with a characteristic critical exponent was predicted [40,45].

Renormalization group (RG), Monte Carlo (MC) calculations and an analogy with the strings predict that the mean separation between membranes diverges as temperature approaches a critical temperature  $T_c$ ,

$$d_w \approx |T - T_c|^{-\psi}, \quad (7)$$

where the universal exponent  $\Psi \approx 1$  [40,45,47–49]. A two-state model for this unbinding transition has been proposed [50]. Membranes can exhibit two different local states: unbound and bound. The probabilities of these two local membrane configurations depend on the temperature, and, at  $T_c$ , membranes are completely unbound [50]. The main conclusions of Refs. [40,45] have been confirmed later in theoretical works [51–53]. In particular, mean field treatments of unbound  $n$  layers confirmed the critical character of the transition and yielded the universal exponent  $\Psi = 1$  [52,53].

An interesting prediction was made in Ref. [53]. It was shown that separation of the stack of membranes to an infinite intermembrane distance is interrupted by a transition to an isotropic “sponge” phase, in which a simple topology of the stack of bilayers is replaced by a locally smooth but randomly connected interface.

It should be noted that some theoretical models differ in their conclusions. Indeed, another approach based on the application of MC techniques to symmetric and asymmetric stacks of  $N$  membranes predicts that in symmetric case all  $N$  membranes unbind simultaneously at  $N$ -independent temperature but with an  $N$ -dependent critical exponent. In the asymmetric case, in which the lowest membrane acts as a rigid wall, they are subjected to a sequence of unbinding transitions with a universal exponent [54].

As it is known, RG calculations can predict the exact value of the critical exponent but give only a rough estimate of the critical temperature. An accurate prediction of  $T_c$ ,

however, is not the only problem. As was mentioned earlier, the values of the bending rigidity and the Hamaker constant have not yet been determined with a proper accuracy. In addition, there is a major disagreement between experimental and theoretical estimates of the  $c_{fl}$  constant, which defines the strength of the undulation force. Also, the uncertainties about the origin of the short-range repulsive forces between membranes mentioned above should be added to the list of the challenges of an accurate prediction of the critical temperature.

In the present situation, a rough estimate of the unbinding temperature of uncharged phospholipid membranes using the superposition of the forces, Eq. (6), yields an enormous spread in the values of  $T_c$  extending from room temperature to more than 1000 K. Obviously, such an estimation does not even answer the question whether the unbinding transition can take place at temperatures at which the membranes still exist.

Experimental studies of the change in the balance of intermembrane interactions (unbinding and adhesion of electrically neutral lipid membranes) led to controversial conclusions. Phospholipid membranes, in particular DMPC, were studied in a large excess of water above the chain-melting phase transition by phase contrast microscopy. It was observed that membranes swell and usually disintegrate forming giant, usually unilamellar, vesicles [55–59]. However, measurements of the vesicles interactions via micropipette aspiration technique yielded a positive value for the adhesion energy,  $(0.01–0.015) \times 10^{-3} \text{ J m}^{-2}$  in the case of phospholipids including DMPC [60,61]. An explanation for this discrepancy was proposed in Refs. [60,61]. It was argued that the micropipette aspiration technique mechanically disturbs the vesicles and may induce tension. It is known that induced tension can suppress membrane undulations and prompt the adhesion of vesicles [57–59]. On the other hand, even if this is true, the well-established fact that uncharged lipids in excess water display x-ray and neutron diffraction peaks (confirming the multilamellar ordered structure of membranes) [11] remains to be explained.

The only example of the unbinding transition in freely suspended membranes was observed with digalactosyl diacylglycerol (DGDG) lipid membranes in an aqueous solution containing 100 mM of NaCl, for which a spontaneous mutual adhesion was observed at low temperature [62]. The unbinding transition did exhibit continuous character. Unfortunately, this observation was made by phase contrast microscopy and quantitative description of the phenomenon was not possible.

Discontinuous thermal unbinding was claimed to have been observed in the highly oriented multilamellar phospholipid membranes from 1-palmitoyl-2-oleoyl-*sn*-glycero-3-phosphatidylcholine and DMPC on silicon substrates [63]. The experiments were done using the x-ray reflectivity method. It is quite possible that interactions of the membrane stack with the substrate partially suppress the undulation in the whole stack as it is described in Ref. [64] and consequently results in the change of the unbinding behavior.

Thus, in spite of important progress, some fundamental problems related to the intermembrane interactions remain unsolved. The nature of the membrane unbinding, the value

of the undulation force constant  $c_{fl}$ , as well as the contribution of the undulations to the balance of intermembrane interactions are clearly among the most important to be studied. However, as we have seen, it is difficult to address them theoretically as well as experimentally. A different approach to the problems under discussion is proposed in this work. It makes use of the power of combined SANS and HRXRD techniques in application to the study of the temperature dependence of the balance of intermembrane forces. As was shown earlier, the undulation force strongly increases with temperature. On the other hand, the van der Waals attraction has only a linear dependence on temperature. In addition, the van der Waals force decreases faster with increase in the intermembrane distance, and therefore one can expect a rapid increase in the strength of the undulation force relative to the van der Waals attraction with a rise in temperature.

How can short-range forces influence this temperature effect? It depends on the nature of the dominant component. A protrusionlike force always helps the undulation force to increase the intermembrane distance with increasing temperature. However, the hydration force itself is expected to act in the opposite way. Consequently, the study of the thermal dependence is, in addition, a test of the origin of the short-range repulsive forces.

Finally, a strong argument in favor of the investigation of temperature dependence of the balance of forces is given by recent experimental observations of the considerable increase in the DMPC intermembrane distance  $d_w$  at temperatures above 65 °C [17,65]. It was stressed in Ref. [17] that the increase in  $d_w$  was accompanied by a dramatic decrease in the intensity of the diffraction peaks. This suggests that in order to account for this effect one has to assume a considerable increase in the amplitude of undulations with temperature [17].

A detailed study of the balance of intermembrane interactions in a wide range of temperatures (from ~40 to 110 °C) has been accomplished in the present work. SANS was employed to accurately determine the thickness of the bilayers, the intermembrane distance [31,62], and the membrane morphology, as well as the dependence of these parameters on temperature. Complementary use of HRXRD at a synchrotron source allowed us to study the thermal evolution of the shape and intensity of diffraction peaks and to determine temperature dependence of undulations. These studies have shown that the membrane unbinding starts at  $T \geq 77$  °C and is clearly visible at higher temperatures. The unbinding progresses continuously and in accordance with the two-state model, as was predicted in Refs. [50,52]. The experimental data allow an estimate of the value of  $c_{fl} = 0.111 \pm 0.005$  to be made, which is in good agreement with all recent theoretical estimations [9,31–38,40,41].

### III. MATERIALS AND METHODS

#### A. Sample preparation

All samples were made from 1,2-dimiristoyl-*sn*-glycero-3-phosphatidylcholine (DMPC) purchased from Sigma (Deisenhoven, Germany). Two types of samples (multilamellar and single membranes) were used for the SANS

study. Multilamellar membranes were prepared by two different methods. In the first method, the lipids were dissolved in ethanol, which was then evaporated by a stream of nitrogen and the rest of the solvent was removed by subjecting a thin lipid film to a high vacuum over a period of several hours. Multilamellar membranes [2% (w/w) of lipid means 2% of lipid by weight] were mixed with heavy water (D<sub>2</sub>O) and homogenized by cycling the sample through the chain-melting phase transition temperature accompanied by vortex mixing.

The second method of preparation consisted in direct dissolution of the lipid powder in D<sub>2</sub>O, keeping the solution at a temperature of ~40 °C for several hours, followed by homogenization as described above. This was done to exclude the possible influence of the residual solvent on the results.

Multilamellar DMPC membranes [30% (w/w) lipid in D<sub>2</sub>O] for x-ray measurements were prepared by the second method. In addition, several cycles of freezing and thawing were done to ensure better homogeneity.

Single vesicles for SANS were prepared by extrusion of liposomes. Multilamellar membranes [2% (w/w) in D<sub>2</sub>O] were pushed through a 100-nm filter using a syringe type extruder (Mensch, Germany) as described in Ref. [66]. The samples were then centrifuged at 13 000 rpm for 1 h to remove the residual multilamellar membranes. This procedure resulted in single vesicles with an average diameter ~80 nm [66].

#### B. Small-angle neutron scattering

SANS measurements were done at the PAXE instrument, Léon Brillouin Laboratory, Saclay, France [67], using a neutron wavelength  $\lambda = 6$  Å, two-dimensional position-sensitive detector at a sample-to-detector distance of 3 m and standard collimation. To determine temperature dependence of the intermembrane distance, SANS measurements of multilamellar and single membranes [both at 2% (w/w) of lipids in D<sub>2</sub>O] were done in parallel. Samples were inserted into a temperature regulated sample holder and measurements were done in the temperature interval from ~40 to 110 °C.

The repeat distance  $d$  of the multilamellar stack was calculated from the position of the diffraction peak maximum in accordance with the Bragg equation  $2d \sin \theta = \lambda$ , where  $\theta$  is half of the scattering angle.

The membrane thickness was determined from SANS measurements of single membranes as described in Refs. [17,67–69]. Briefly, the scattering intensity  $I(Q)$  of noninterfering single membranes in dilute samples is described by the Kratky-Porod approximation [67–69]:

$$I(Q) = Q^{-2} I(0) \exp[-R_g^2 Q^2], \quad (8)$$

where  $Q$  is the scattering vector ( $Q = 4\pi \sin \theta / \lambda$ ),  $R_g$  is the radius of gyration of the membrane thickness:

$$R_g^2 = \frac{\int [\rho_m(x) - \rho_s] x^2 dx}{\int [\rho_m(x) - \rho_s] dx}, \quad (9)$$

$\rho_m(x)$  is the neutron scattering length density along the direction  $x$  normal to the membrane,  $\rho_s$  is the scattering length density of the solvent, and

$$I(0) = \sum n_i (\overline{\rho_m} - \rho_s)^2 V_i^2, \quad (10)$$

where  $n_i$  is the number of membranes with the volume  $V_i$ ,  $\overline{\rho_m}$  is the average neutron scattering length density of membranes. Equation (8) is valid in the range  $1/R_v \leq Q \leq 1/R_t$  [17,67–69], where  $R_v$  is the radius of the vesicles.

Membrane thickness can be obtained from a contrast variation study using  $D_2O$  to  $H_2O$  substitution. The radius of gyration  $R_t$  of a flat object in a solvent depends on the contrast  $\Delta\rho = \rho_m - \rho_s$  as

$$R_t^2 = R_c^2 + (\overline{\rho_m}/\Delta\rho)(R_p^2 - R_c^2 + L^2) - (\overline{\rho_m}/\Delta\rho)^2 L^2, \quad (11)$$

where  $R_c$  is the radius of gyration of the membrane inaccessible by the solvent,  $R_p$  is the radius of gyration of the membrane [ $R_p$  can be calculated using Eq. (9) with  $\rho_s=0$ ],  $L$  is the distance between geometric and neutron scattering density centers of gravity [68]. In the case of a centrosymmetrical membrane (like the DMPC membrane)  $L=0$ , and Eq. (11) simplifies to

$$R_t^2 = R_c^2 + \frac{\overline{\rho_m}}{\Delta\rho}(R_p^2 - R_c^2). \quad (12)$$

Equation (12) is used to fit the dependence of measured  $R_t^2$  on  $\overline{\rho_m}/\Delta\rho$  by a straight line to obtain the  $R_c$ . In the case when there is no water penetration into membrane, the membrane thickness can be calculated simply as  $d_b = \sqrt{12}R_c$  [68,69]. It is well known, however, that water does penetrate into the polar part of the lipid membrane [70] and we will take into account this fact here to estimate a correction to the above formula.

The real thickness of the membrane  $d'_b$  can be determined from

$$\frac{d'_b{}^2}{12} = \frac{V_L}{V_L + V_W} R_c^2 + \frac{V_W}{V_L + V_W} R_W^2, \quad (13)$$

where  $V_L$  and  $V_W$  are the volumes of DMPC molecule and the volume of water inside of the membrane, respectively,  $R_W$  is the radius of gyration of the part of the bilayer that is filled with water. In order to determine  $R_W$ , we assume a linear distribution of water in the polar region of the membrane [71–73], which results in

$$\begin{aligned} R_W^2 &= \frac{\int_{d'_b/2-D_H}^{d'_b/2} \left[ x - \left( \frac{d'_b}{2} - D_H \right) \right] x^2 dx}{\int_{d'_b/2-D_H}^{d'_b} \left[ x - \left( \frac{d'_b}{2} - D_H \right) \right] dx} \\ &= \frac{d'_b{}^2}{12} \left[ 3 - 4 \frac{D_H}{d'_b} + 2 \left( \frac{D_H}{d'_b} \right)^2 \right], \end{aligned} \quad (14)$$

where  $D_H$  is the thickness of the hydrophilic part of the bilayer. Substitution of  $D_H=9 \text{ \AA}$  [70,74] and combining Eqs. (13) and (14) result in

$$d'_b = d_b \left( 1 - 1.26 \frac{V_W}{V_L} \right)^{-1/2} = 1.15 d_b, \quad (15)$$

where  $V_W = n_W V_{WL} = 7.2 \times 30 \text{ \AA}^3 = 216 \text{ \AA}^3$  [70,74]. Equation (15) will be used to determine the membrane thickness  $d'_b$  at all of the measured temperatures.

Unfortunately, a detailed study of the temperature dependence of  $d'_b$  by the contrast variation method would require a significant amount of neutron beam time. For this reason we have used another approach to determine the temperature dependence of the membrane thickness. From Eq. (12) one can see that when  $|\Delta\rho| \gg \overline{\rho_m}$  the measured in a single experiment  $R_t$  is very close to  $R_c$ . The highest contrast is achieved when measurements are done in  $D_2O$ . The neutron scattering density of  $D_2O$  is equal to  $\rho_s = 6.38 \times 10^{10} \text{ cm}^{-2}$  and the average neutron scattering density of DMPC membrane is  $\overline{\rho_m} = 0.282 \times 10^{10} \text{ cm}^{-2}$  at  $T=30 \text{ }^\circ\text{C}$  ( $\overline{\rho_m}$  was calculated using partial volume  $V=1097 \text{ \AA}^3$  of the DMPC molecule [70]). Equation (12) can be rewritten as

$$R_c^2 = R_t^2 \left\{ \frac{1 - \frac{\overline{\rho_m}}{\Delta\rho} \frac{R_p^2}{R_t^2}}{1 - \frac{\overline{\rho_m}}{\Delta\rho}} \right\}. \quad (16)$$

The ratio  $\overline{\rho_m}/\Delta\rho$  is small (it is equal to 0.04 for DMPC membranes in  $D_2O$ ) and has a very weak temperature dependence (volume thermal expansivities of lipid and water molecules at  $50 \text{ }^\circ\text{C}$  have small and very close values, which are equal to  $5.1 \times 10^{-4}$  and  $4.5 \times 10^{-4} \text{ K}^{-1}$ , correspondingly [75]). In addition, the ratio  $R_p^2/R_t^2$  has a weak temperature dependence as well and the reason for this is that the both values  $R_p^2$  and  $R_t^2$  originate from the same structural parameters of the bilayer. Therefore temperature dependence of the second term in the right hand side of Eq. (16) is negligible and one can use the following approximation for estimation of  $R_c$  from measured  $R_t$  at a temperature  $T$ :

$$R_c(T) = R_t(T) \frac{R_{c,T_1}}{R_{t,T_1}}, \quad (17)$$

where  $R_{c,T_1}$  and  $R_{t,T_1}$  are the radii of gyration obtained from a contrast variation study at temperature  $T_1$  according to Eq. (12). In other words, it is sufficient to determine  $R_c$  at a single temperature  $T_1$  in order to find membrane thickness at any other temperature, at which  $R_t$  was measured. In case of DMPC membranes in  $D_2O$ , when using the approximation from Eq. (17), the membrane thickness errors in the whole studied temperature interval do not exceed  $0.2 \text{ \AA}$ .

## C. High-resolution x-ray diffraction

### 1. HRXRD measurements

The experiments were performed on the small-angle x-ray scattering (SAXS) instrument of the high brilliance ID2 beam line at the European Synchrotron Radiation Facilities (ESRF, Grenoble, France) [76]. A wavelength of  $1 \text{ \AA}$  was used for the measurements. To achieve the highest possible resolution of the instrument a two-dimensional gas wire

x-ray detector was moved to the maximum possible distance from the sample, 10 m, and shifted from the beam center to the position of the first order reflection. The x-ray beam was focused at the detector position. The size of the beam on the sample was  $0.3 \times 0.3 \text{ mm}^2$ . The experimentally obtained resolution function of the instrument (Fig. 8) is well approximated by the sum of two Gaussians:

$$R(\Delta q) = A_1 e^{-(\Delta q)^2/2\delta_1^2} + A_2 e^{-(\Delta q)^2/2\delta_2^2} \quad (18)$$

with  $A_2/A_1 = 1/3$ ,  $\delta_1 = 3.3 \times 10^{-4} \text{ \AA}^{-1}$ , and  $\delta_2 = 9.9 \times 10^{-4} \text{ \AA}^{-1}$ . The full width at half maximum of the resolution function is  $\sim 10^{-3} \text{ \AA}^{-1}$ .

The study was done with nonoriented DMPC membranes in excess  $\text{D}_2\text{O}$  [30% (w/w) of DMPC]. Samples were placed in a thin, cylindrical aluminum cell and confined by two parallel thin mica windows attached on both sides of a 2-mm spacer. The measurements were done at temperatures 48.6, 58.0, 67.4, 76.8, 85.7, 89.7, and 95.4 °C. Temperature was controlled with an accuracy of  $\pm 0.1$  °C. An incubation of at least 30 min was applied before measurements at each temperature.

Radiation damage effects were carefully examined by monitoring the stability of the diffraction peaks (both intensity and shape) while continuously irradiating the sample with series of 10-s exposures. As a result of this study the flux was reduced to  $\sim 10^{11} \text{ photons mm}^{-2}$  and the exposure time was limited to 1 min. In addition, after each 1-min exposure the sample was shifted by 1 mm in vertical or horizontal direction to a fresh position and an additional short, 10-s, exposure was taken. Finally, the reproducibility of the measurements and equilibration and stability of the samples were checked by an additional set of measurements in the cooling direction. The shape and intensity of the diffraction peaks obtained at the same temperatures in the heating and cooling directions were identical, within experimental accuracy, in all cases.

## 2. Analysis of the diffraction peak shape

Intensity of the x-ray scattering from a smectic liquid crystalline sample can be expressed as

$$I(Q) = |F(Q)|^2 S(Q), \quad (19)$$

where  $F(Q)$  is the form factor of a single smectic layer and  $S(Q)$  is the structure factor, which depends on the spatial correlation between layers in the sample. The structure factor is defined as a Fourier transform:

$$S(\mathbf{Q}) = \int d\mathbf{R} G(\mathbf{R}) \exp(i\mathbf{Q} \cdot \mathbf{R}) \quad (20)$$

of the main-correlation function

$$G(\mathbf{R}) = \langle \exp(i\mathbf{Q} \cdot \mathbf{n}[u(\mathbf{R}) - u(0)]) \rangle, \quad (21)$$

where  $\mathbf{n}$  is the unit vector normal to the smectic layers and  $u(\mathbf{R})$  is the layer displacement in the direction  $\mathbf{n}$  at the position  $\mathbf{R}$ . The brackets  $\langle \rangle$  denote the thermal averaging.

Caillé [77] showed that using the standard harmonic approximation and de Gennes free energy [Eq. (5)], the struc-

ture factor of a nonoriented smectic sample in the vicinity of the diffraction peak maximum  $Q_0$  can be approximated as

$$S(Q) \propto |Q - Q_0|^{-1+\eta}, \quad (22)$$

where  $\eta$  is the so-called Caillé parameter, defined by

$$\eta = Q_0^2 \frac{k_B T}{8\pi\sqrt{BK}}. \quad (23)$$

Equation (22) implies that when the Caillé parameter is larger than 1 (either at large  $Q$  or at low  $B$  and  $K$ ), the diffraction peaks become nonobservable. Thus one-dimensional translational order in a system of multilayer membranes is destroyed by thermal fluctuations (undulations) and this results in a power law decay of the intensity in the vicinity of the diffraction peak maximum. Such an algebraic decay of the positional order in smectic crystals was predicted by Landau [78] and Peirls [79], observed by Als-Nielsen *et al.* [80], and was studied experimentally for different oriented and nonoriented liquid crystals. More recently, theoretical and experimental investigations of this phenomenon, in application to lipid multilayers, were done by Nagle *et al.* [74,81–83].

It should be noted that the shape of the diffraction peak given by Eq. (22) is symmetrical. Asymmetry of the peaks can be deduced in the next level of approximation [84]:

$$S(Q) \propto |Q - Q_0|^{-1+\eta} \left[ \sin\left(\frac{1}{2}\pi\eta\right) + \frac{\eta}{2\xi Q_0} \times \text{sgn}(Q - Q_0) \cos\left(\frac{1}{2}\pi\eta\right) \right], \quad (24)$$

where the parameter  $\xi = \sqrt{K/B}$  is called the penetration length. However, the asymmetry is only observable when  $\xi < 2\pi/Q_0$  [42,43,84].

Fitting the experimental diffraction peak profiles in this study was done following the so-called modified Caillé theory [81] with one following addition. It is widely assumed that the lipid bilayer form factor  $F(Q)$  is practically constant in the narrow region of the high resolution diffraction peaks and therefore it is omitted from the analysis [42–44,74,81–83]. In this work we have demonstrated that this is not always true and that the form factor can have a significant effect on the tails of the diffraction peaks (see Sec. IV B). Thus the shapes of the peaks, after background subtraction, correction for the Lorenz factor, and correction for the form factor, were fitted by Eq. (80) from Ref. [81] (see Appendix A), convoluted with the instrumental resolution function defined by Eq. (18). Nonlinear least square fits of the data curves were done using the MINUIT library [85] from the CERNLIB package. The free fitting parameters were the parameter  $\eta$ , the mean size of the domains  $L_0$ , and the domains distribution  $\sigma_L$ .

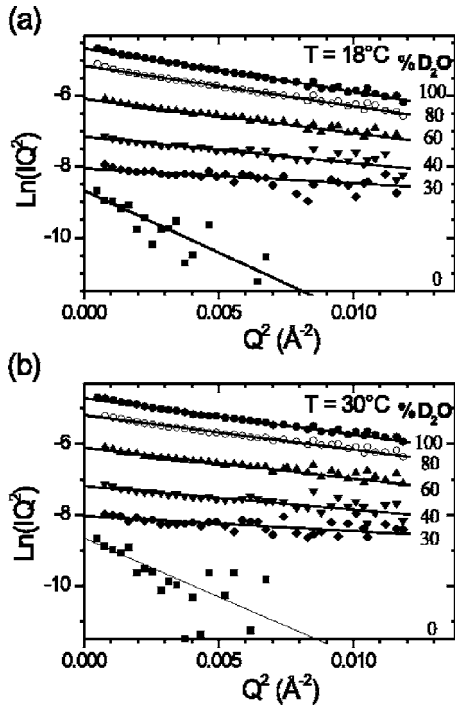


FIG. 1. SANS curves from 2% (w/w) DMPC single membranes in different contrasts ( $\text{H}_2\text{O}/\text{D}_2\text{O}$  ratios) are shown using the Kratky-Porod presentation [ $\text{Ln}(IQ^2)$  vs  $Q^2$ ] at  $18^\circ\text{C}$  ( $P_{\beta'}$  phase) (a) and at  $30^\circ\text{C}$  ( $L_{\alpha}$  phase) (b). Straight lines are fits using Eq. (8).

#### IV. RESULTS AND DISCUSSION

##### A. Small-angle neutron scattering

###### 1. Temperature dependence of the membrane thickness

Studies of intermembrane interactions require an accurate determination of the membrane structural parameters. Therefore we performed a detailed SANS study with single DMPC vesicles to obtain the membrane thickness and its temperature dependence. Typical small-angle scattering curves at temperatures  $T=18^\circ\text{C}$  ( $P_{\beta'}$  phase) and  $T=30^\circ\text{C}$  ( $L_{\alpha}$  phase) are shown in the Kratky-Porod representation  $\text{Ln}(IQ^2)$  vs  $Q^2$  (Fig. 1). A linear fit yields the value of the radius of gyration, which is related to the membrane thickness.

In preparation for the temperature measurements, we evaluated the influence of possible intervesicle interference and membrane curvature on the accuracy of the method. For this purpose SANS measurements were performed at different concentrations and curvatures (vesicle sizes) of the membranes. The results are summarized in the Tables I and II.

Data show that within the experimental accuracy there are no significant effects of either intervesicle interference or curvature in the tested range of concentrations and vesicle sizes. Thus samples with 2% (w/w) lipid concentration and  $D=100$  nm were chosen for the rest of the measurements.

The next step was to perform a SANS contrast variation study at  $T=18$  and  $30^\circ\text{C}$  in order to obtain  $R_c$  [see Eq. (12)] that will be used to determine the membrane thickness. The Kratky-Porod plots at temperatures 18 and  $30^\circ\text{C}$  and different contrasts are shown in Fig. 1. The data allowed us to obtain accurate values for  $R_c$  at both temperatures. The re-

TABLE I. Dependence of the membrane thickness (estimated as  $\sqrt{12}R_t$ ) of DMPC membranes in  $\text{D}_2\text{O}$  at  $30^\circ\text{C}$  on the lipid concentration.

DMPC concentration (% w/w)	Membrane thickness $\sqrt{12}R_t$ ( $\text{\AA}$ )
0.5	$34.8 \pm 0.3$
1	$35.3 \pm 0.4$
2	$35.0 \pm 0.4$
4	$35.1 \pm 0.4$

sults of the fits using Eq. (12) are shown in Figs. 2 and 3 and summarized in the Table III.

The accuracy in  $\rho_m$  is not very high, but the experimental values agree within errors with  $\rho_m=0.297 \times 10^{10} \text{ cm}^2$  ( $T=18^\circ\text{C}$ ) and  $\rho_m=0.282 \times 10^{10} \text{ cm}^2$  ( $T=30^\circ\text{C}$ ) as calculated from the partial volumes of DMPC molecules  $V_L=1044 \text{ \AA}^3$  in the gel phase and  $V_L=1097 \text{ \AA}^3$  in the liquid crystalline phase [70]. The membrane thickness, estimated from  $d_b = \sqrt{12}R_c$ , assuming no water penetration in the membrane, yields  $d_b=41.1 \pm 0.4 \text{ \AA}$  at  $18^\circ\text{C}$  in the gel phase and  $37.9 \pm 0.3 \text{ \AA}$  at  $30^\circ\text{C}$  in the liquid phase. This latter value can be compared with  $38.1 \pm 1.0 \text{ \AA}$ , obtained from the linear extrapolation to  $30^\circ\text{C}$  of data ( $d_b=35.3 \pm 1.0 \text{ \AA}$  at  $31.8^\circ\text{C}$ )  $d_b=36.3 \pm 1.0 \text{ \AA}$  at  $31.7^\circ\text{C}$ , and  $d_b=39.5 \pm 1.0 \text{ \AA}$  at  $27^\circ\text{C}$ ) from a similar contrast variation study with DMPC membranes [69]. Correction for the water penetration effect using Eqs. (14) and (15) yields the steric membranes thickness  $d'_b=43.7 \pm 0.4 \text{ \AA}$  at  $30^\circ\text{C}$ . This value coincides with the best estimate of  $44.2 \text{ \AA}$  [70] and  $44.5 \pm 0.3 \text{ \AA}$  [91] and close to the result  $d'_b=42.6 \pm 0.5 \text{ \AA}$  of recent computer simulations of SANS contrast variation data by a multishell model of bilayer neutron scattering length density [86].

Measurements of the temperature dependence of the membrane thickness were done in the temperature interval from  $46$  to  $104^\circ\text{C}$ . The radius of gyration of the membrane  $R_t$  was determined as described in Sec. III B and the bilayer thickness  $d'_b$  was obtained using Eq. (15), where  $R_c(T)$  was estimated from Eq. (17) using values of  $R_t(T)$ ,  $R_{c,T_1}$ , and  $R_{t,T_1}$  determined from contrast variation study at  $30^\circ\text{C}$ . It is worth mentioning that Eq. (15) was used to correct the bilayer thickness for water penetration into the polar part of the membrane at different temperatures. This correction depends

TABLE II. Dependence of the membrane thickness (estimated as  $\sqrt{12}R_t$ ) of DMPC membranes in  $\text{D}_2\text{O}$  at  $T=18$  and  $30^\circ\text{C}$  on the vesicle size ( $D$  is the average diameter of the pore in nuclear membranes used for the sample preparation. It provides a rough estimation of the vesicle diameter [65]).

Sample	$\sqrt{12}R_t$ ( $\text{\AA}$ )		
	$D=50$ nm	$D=100$ nm	$D=200$ nm
DMPC, $T=18^\circ\text{C}$ ( $P_{\beta'}$ phase)	$36.8 \pm 0.3$	$38.3 \pm 0.1$	$38.3 \pm 0.3$
DMPC, $T=30^\circ\text{C}$ ( $L_{\alpha}$ phase)	$35.7 \pm 0.4$	$35.2 \pm 0.3$	$35.8 \pm 0.4$

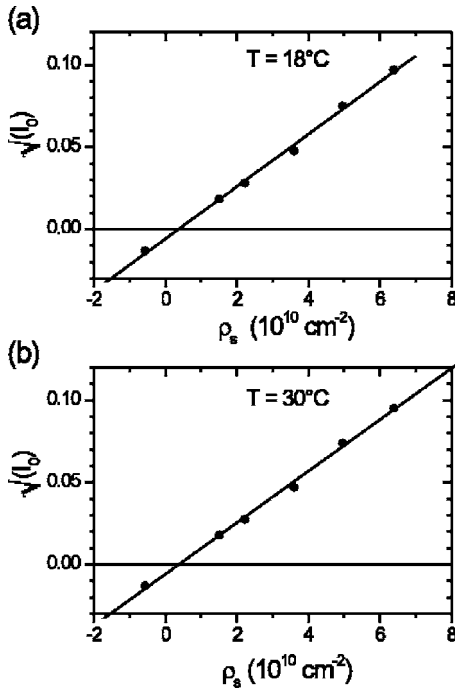


FIG. 2. Dependence of the square root of SANS intensities at zero angle  $I(0)$ , obtained from fitting curves shown in Fig. 1, on the solvent neutron scattering length density at 18 °C ( $P_{\beta'}$  phase) (a) and 30 °C ( $L_{\alpha}$  phase) (b). Intersection of the straight fit line with the abscissa axis ( $y=0$ ) gives the value of the mean lipid membrane neutron scattering length density  $\rho_m$ .

on the ratio  $V_W/V_L$ , which, in its turn, changes with temperature. Therefore we have attempted a proper correction for temperature dependence of  $V_W/V_L$  (the procedure of the correction is described in Appendix B). Equations (13), (15), and (B3) were used to determine the thickness of DMPC bilayer. It is interesting to note that the value of this correction is relatively small in the whole studied range of the temperatures (i.e., it is equal to 0.36 Å at 77 °C). Temperature dependence of the corrected membrane thickness is shown in Fig. 4. Membrane thickness decreases roughly linearly with temperature. The thermal compression of the bilayer thickness  $\Delta d_b'/\Delta T$  in the temperature interval from 46 to 104 °C is equal to  $0.058 \pm 0.003$  Å K<sup>-1</sup>.

## 2. SANS from multilamellar DMPC membranes: Temperature dependence

The measurements were performed with 2% (w/w) of DMPC membranes in D<sub>2</sub>O. The main differences of this study from other similar studies [17,65] are as follows:

- (i) the measurements were extended to higher temperatures (up to  $\sim 110$  °C), and
- (ii) the scattering intensity was measured and analyzed not only in the vicinity of the multilamellar diffraction peak ( $Q \sim 0.1$  Å<sup>-1</sup>) as in Refs. [17,65], but also at lower  $Q$  (from 0.01 to 0.3 Å<sup>-1</sup>).

The scattering curves at some of the measured temperatures are shown in Fig. 5. They display a shift of the diffraction peak to smaller  $Q$  values (larger repeat distances  $d$ ), a decrease of the integral intensity of the peak, and its broad-

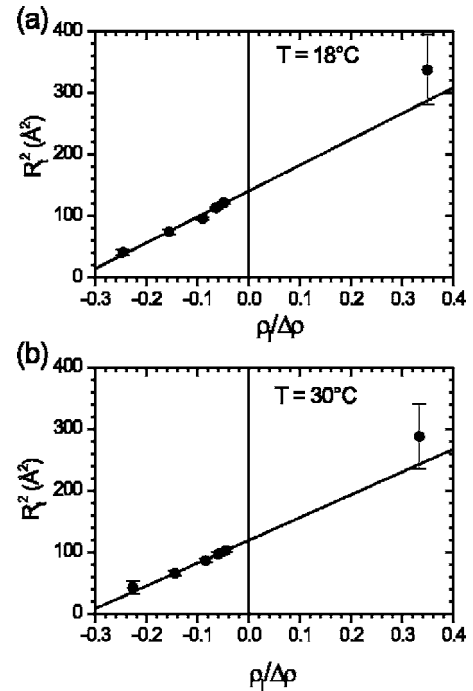


FIG. 3. Dependence of the square of the radius of gyration of DMPC membranes on  $\rho_m/\Delta\rho$  at 18 °C ( $P_{\beta'}$  phase) (a) and 30 °C ( $L_{\alpha}$  phase) (b). Intersection of the straight fit line with the ordinate axis ( $x=0$ ) gives the value of the radius of gyration in infinite contrast  $R_c$ .

ening at higher temperatures. In addition, a striking increase in the small-angle scattered intensity at temperatures  $T \geq 77$  °C is observed. The scattered intensity  $I(Q)$  was fitted by the function

$$I(Q) = I_f(0)Q^{-2} \exp[-R_f^{*2}Q^2] + I_0 \exp\left[-\frac{(Q-Q_0)^2}{2\sigma_Q^2}\right], \quad (25)$$

where the first component is the small-angle contribution and the Gaussian function describes the diffraction peak.  $I_f(0)$ ,  $R_f^*$ ,  $I_0$ ,  $Q_0$ , and  $\sigma_Q$  are the fitting parameters. It should be noted that Eq. (25) is an approximation of Eq. (19). The first term in the right side of this equation corresponds to the

TABLE III. Parameters of DMPC membranes calculated from the fit [Eq. (12)] of the contrast variation data.  $\bar{\rho}_m$  is the average neutron scattering density of the membranes,  $R_c^2$  is the radius of gyration of the membrane at infinite contrast, and  $R_p^2 - R_c^2$  is the parameter, that characterizes the neutron scattering density distribution inside the membrane.

Sample	$\bar{\rho}_m$ (10 <sup>10</sup> cm <sup>-2</sup> )	$R_c^2$ (Å <sup>2</sup> )	$R_p^2 - R_c^2$ (Å <sup>2</sup> )
DMPC, $T=18$ °C ( $P_{\beta'}$ phase)	$0.37 \pm 0.10$	$141.0 \pm 2.8$	$423 \pm 31$
DMPC, $T=30$ °C ( $L_{\alpha}$ phase)	$0.36 \pm 0.10$	$119.6 \pm 1.7$	$369 \pm 21$

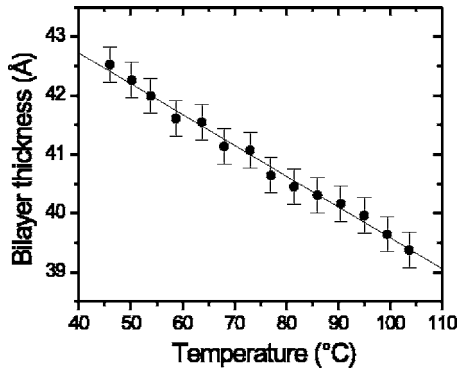


FIG. 4. Temperature dependence of the DMPC membrane thickness obtained from SANS experiments. Linear fit gives thermal compression of the bilayer,  $\Delta d_b'/\Delta T = 0.058 \pm 0.003 \text{ \AA K}^{-1}$ .

Kratky-Porod approximation for the scattering intensity from single lamellar [see Eq. (8)]. The second term corresponds to a correlation peak for a stack of membranes. The temperature dependence of the repeat distance ( $d = 2\pi/Q_0$ ), the width of the peak  $\sigma_Q$ , and the radius of gyration of membrane  $R_g^*$  are shown in Figs. 6(a)–6(c), respectively. Both dependences of  $d$  and  $\sigma_Q$  qualitatively exhibit the same behavior in response to temperature. Above a temperature of  $\sim 77^\circ\text{C}$ , both the repeat distance and the width of the diffraction peak increase progressively with temperature. On the other hand,  $R_g^*$  decreases dramatically with temperature. At higher temperatures, the small-angle part of the scattering approaches the scattering curve from single membranes and coincides with it, as is seen in Fig. 5. The slope of this part of the scattering curve yields the correct thickness of the bilayer. Observed in the current work, the dependence of the repeat distance on  $T$  agrees within experimental accuracy with measurements in the literature [17,65] made in the common temperature range.

The width of the diffraction peak  $\sigma_Q$  depends on both the instrumental resolution  $\sigma_{iQ}$  and the diffraction contribution from the sample,  $\sigma_{sQ}$ :

$$\sigma_Q^2 = \sigma_{sQ}^2 + \sigma_{iQ}^2. \quad (26)$$

The plateau at low temperatures [Fig. 6(b)] is determined solely by the instrumental resolution  $\sigma_{iQ}$  and allows its esti-

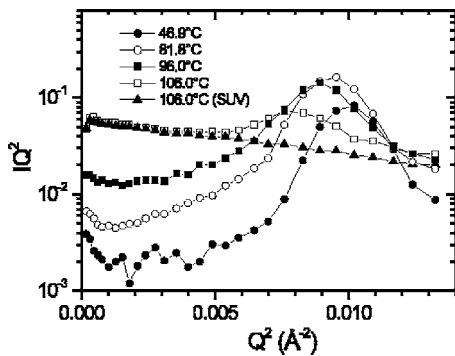


FIG. 5. SANS curves from 2% (w/w) multilamellar DMPC membranes in  $\text{D}_2\text{O}$  at different temperatures and from 2% (w/w) single DMPC membranes in  $\text{D}_2\text{O}$  at  $T = 106^\circ\text{C}$  are shown in the Kratky-Porod representation.

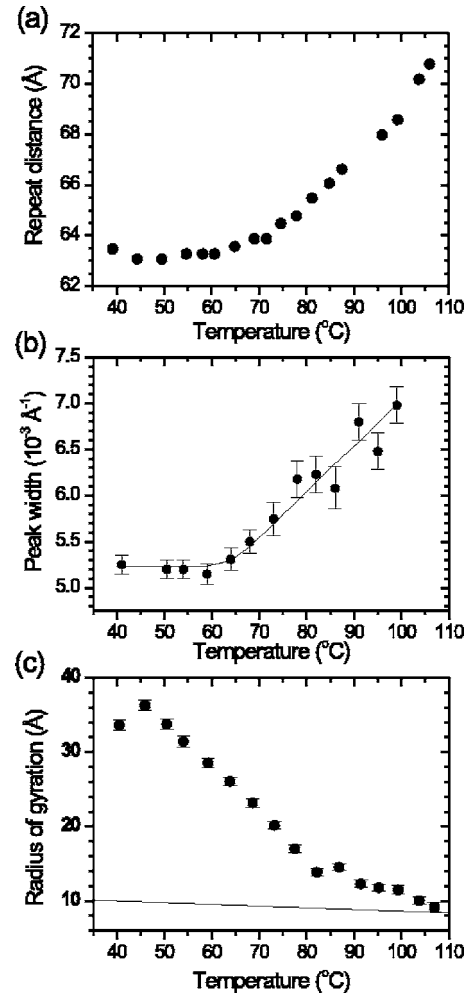


FIG. 6. Temperature dependences of the multilamellar DMPC membrane repeat distance (a), of the width of the diffraction peaks  $\sigma_Q$  (b), and of the “effective” radius of gyration  $R_g^*$  (c) obtained from SANS measurements shown in Fig. 5.

mation. Assuming that the increase in the width of the peak is determined by the finite size effect and that the instrumental resolution does not change significantly in the small  $Q$  range defined by the range in the peak positions, one can find the temperature dependence of the average number of bilayers in multilamellar membranes from the following equation:

$$N \approx \frac{1}{\sqrt[2]{\sigma_Q^2 - \sigma_{iQ}^2}} \frac{\pi}{d}. \quad (27)$$

As it follows from the data shown in Fig. 6(b) the average number of bilayers in the multilamellar stack is reduced considerably at higher temperatures. As an illustration,  $N \approx 60$  at  $T = 60^\circ\text{C}$ ,  $N \approx 30$  at  $77^\circ\text{C}$ , and  $N \approx 8$  at  $98^\circ\text{C}$ .

To summarize, a substantial decrease in the intensity of the diffraction peak with temperature at  $T \geq 77^\circ\text{C}$  is accompanied by the increase in its width and remarkable increase in the small-angle scattering intensity. The small-angle part of  $I(Q)$  approaches that of single DMPC vesicles at higher temperatures. It is important to stress that the analysis of the small-angle part of the scattering curve and the width of the

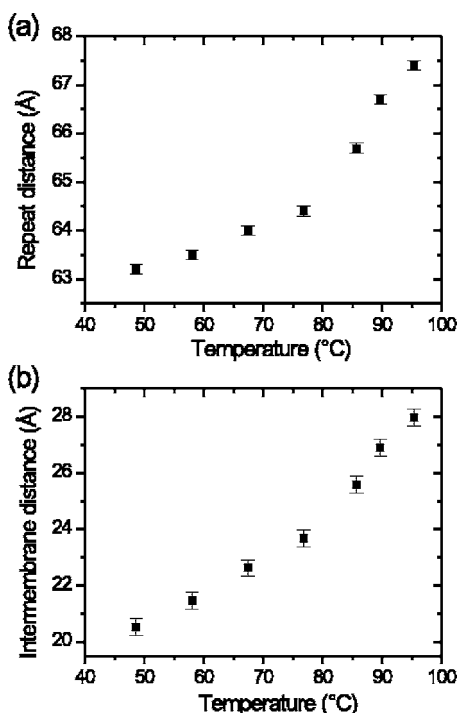


FIG. 7. Temperature dependences of the repeat distance  $d$  of 30 wt % multilamellar DMPC membranes in  $D_2O$  determined from the positions of HRXRD peaks (a); of the bilayer thickness  $d'_b$ , determined from SANS data with single membranes (b), and water spacing  $d_w$ , calculated as  $d_w = d - d'_b$  (c).

peak results in the same conclusion: the average size of the coherent domains decreases with temperature and approaches the thickness of a multilamellar stack containing just a few bilayers at higher temperatures.

Parenthetically, we note that when the sample has been cooled down to 50 °C, the position of the diffraction peak returns back to its initial position. At the same time the integral intensity of the peak rises and the small-angle scattering intensity drops, however, none of the intensities reaches their initial values. We interpret this as evidence that the multilamellar liposomes lost some of their outer bilayers at higher temperatures.

The temperature dependence of the intermembrane distance  $d_w$  calculated as  $d_w = d - d_b$  is shown in Fig. 7(b). As expected, there is a prominent increase in  $d_w$  with temperature, starting from 77 °C.

Therefore the SANS experiments indicate that the unbinding of DMPC membranes starts at  $T \sim 77$  °C and proceeds in agreement with the two-state model, i.e., the volume fraction of the unbound state increases with temperature.

A detailed theoretical discussion of the two-state model is given by Lipowsky in Ref. [50], where probabilities of the “locally bound”  $P_{2b}$  and “locally unbound”  $P_{ub}$  states were introduced. The ratio  $P_{2b}/P_{ub}$  is governed by the interplay of forces acting between membranes and must vanish in a continuous way as the transition temperature  $T_c$  is approached [50]. In our work we experimentally observed the onset of the unbinding transition at  $\sim 77$  °C. When temperature approaches  $T_c$ , the relaxation time of the system also diverges [45]. In this case, kinetics can certainly play a role and spe-

cial precautions need to be taken to obtain accurate value of  $T_c$ . This was not the main thrust of our study. However, we did check evolution of the SANS curves in time at several temperatures above 77 °C and have not detected any significant changes on the time scales of  $\sim 1$  h. The method used in the present work for preparation of the multilamellar membranes gives mostly large and generally not tightly packed liposomes and should not impose strong geometrical restrictions on the number (area) of locally unbound membranes. However, owing to the wide size distribution of the liposomes, a small number of the multilamellar liposomes will have small size and will be tightly packed (onionlike topology). In such liposomes, relaxation of membranes to equilibrium state will require some morphological rearrangements, accompanied by redistributions of lipid molecules between membranes. As a consequence, the number (or area) of the locally unbound membranes will be kinetically dependent. This process would require an especially long time, since it is determined mostly by a slow flip-flop transition of lipids in membranes.

#### B. High-resolution x-ray diffraction: Analysis of the temperature dependence of the shape of diffraction peaks

In the previous section we demonstrated that combined SANS data on multilamellar and unilamellar vesicles show a considerable increase in the intermembrane distance with increase in temperature at  $T \geq 77$  °C and indicate that the unbinding of the membranes starts with further increase in the temperature. Moreover, single membrane SANS data have explicitly shown that the membrane thickness gradually contracts with temperature. As we discussed in the introduction, a reduction in the membrane thickness results in the softening of the membrane and in a decrease of the membrane bending rigidity. This fact together with relatively strong dependence of the undulation force on temperature can lead to a considerable increase in the membrane undulations and shift the balance of the intermembrane forces toward unbinding. However, all these results, while giving evidence of increased undulations, do not prove that directly.

In order to examine the role of undulations in the observed effects directly, we performed a high-resolution x-ray study of the temperature dependence of the undulations at the ID2 beam line at ESRF. The diffraction patterns showing the first order diffraction peak at different temperatures are presented in Fig. 8. Using a two-dimensional position sensitive detector at the small-angle instrument allowed us to collect very high statistical quality high-resolution diffraction data at a minimum level of radiation damage of the samples. There are five general features of the peak. First, the peak widths at all temperatures are considerably larger than the resolution of the instrument. Second, the maximum intensity of the peaks decreases with temperature. Third, the diffraction peak broadens significantly with an increase in temperature. Fourth, the wings of the peak decay slower as temperature rises thus manifesting an increase in the undulations with temperature [42–44]. Finally, the shape of the peak is asymmetric.

To check for reproducibility of the data the measurements were repeated at several temperatures (data not shown), as

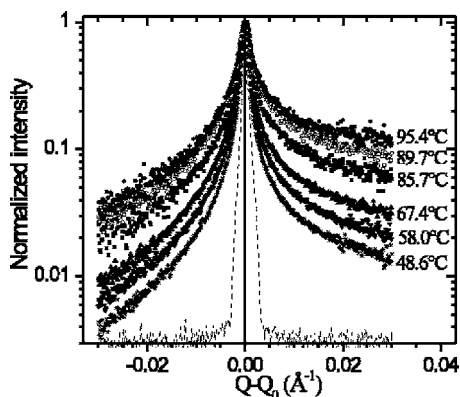


FIG. 8. HRXRD peaks from 30% (w/w) multilamellar DMPC membranes in  $D_2O$  at different temperatures. Intensities of the peaks maxima are normalized to 1. The dash line curve is the resolution of the instrument. The peaks are asymmetric and exhibit long tails.

the sample was cooled. Regardless of the heating or cooling direction, intensity, position, and shape of the diffraction peaks measured at the same temperatures coincide within experimental errors. As has been discussed previously, SANS data also show the same repeat distances after cooling down, however, the intensities of the diffraction peaks as well as intensities of the low angle parts of the scattering curves were clearly different. We suggest that this discrepancy between SANS and HRXRD data is due to the significant difference in the concentrations of lipids in the samples. In the case of SANS experiments, where only 2% (w/w) of the liposomes (lipids) was used, the increased undulation pressure on the external membrane shell in the onion structure of the liposomes is not compensated for by the external pressure and as a consequence the outer membranes can be ruptured. Conversely, in the case of HRXRD experiments, where 30% (w/w) of the lipid was used, the liposomes are already quite densely packed and the external pressure from neighboring liposomes can partially compensate for the internal one. Another reason for the differences could be that the size of the liposomes in the case of HRXRD experiments is much larger than in the SANS experiments and the rupture of outer membranes does not noticeably change the number of the bilayers in the onion.

Temperature dependence of the repeat distance  $d$  as determined from HRXRD and the bilayer thickness  $d_b$  as determined from SANS data as well as intermembrane water spacing  $d_w$  calculated as  $d_w = d - d_b$  are shown in Figs. 7(a) and 7(b) and they agree within experimental errors with the results of the SANS study [Fig. 6(a)].

As we mentioned above, the diffraction peaks are asymmetric. The asymmetry of the intensities of the left and right parts of the peaks has been recognized and discussed in Refs. [42–44]. However, computer modeling shown in Fig. 9 as well as analytical calculations resulting in Eq. (24) [84] mean that the asymmetry can only occur due to a difference in the intensities, but the slopes of the wings of the diffractions peaks (in log-log representation) remain the same. Both parts of the peaks are plotted in log-log representation in Fig. 10 for the data measured at four different temperatures. The

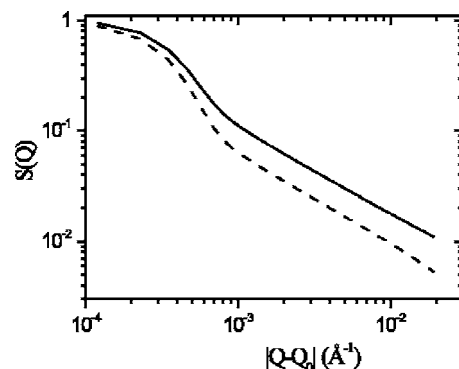


FIG. 9. Computer simulation of the structure factor using Eq. (A3). Left and right parts of the peak exhibit asymmetry in the intensities (but not in the slopes) at small de Gennes penetration length. The calculations were done for  $\eta=0.2$ ,  $\lambda=10 \text{ \AA}$ , and  $L_0=10^4 \text{ \AA}$ .

difference between the left and right parts of the diffraction peaks is already visible at  $q=Q-Q_0=0.003 \text{ \AA}^{-1}$ , but it is more due to the difference in the slopes and not due to the intensity itself. To resolve the discrepancy between theoretical predictions of the same slope for the left and right parts and experimental data, one should take into account behavior of the form factor  $F(Q)$  in the vicinity of the diffraction peak maximum. Usually, the form factor is assumed to be constant in the vicinity of the diffraction peak maximum and analysis of the diffraction peak shape is done without taking into consideration the dependence of the form factor on the scattering vector [42–44,82]. This dependence, however, can be calculated from the known electron density profiles of the DMPC lipid membranes [82] or determined with the help of the Shannon sampling theorem [16,82]. Both approaches give the same result: contribution of  $F(Q)$  to the change of the intensity  $I(Q)$  is already about 20% at  $q=0.01 \text{ \AA}^{-1}$ . Therefore we decided to correct the intensity of the diffraction peaks by the form factor before the analysis of  $S(Q)$ . The correction was done in the first approximation assuming a linear dependence of the form factor on  $q$  in the vicinity of the position  $Q_0$  of the diffraction peak maximum:

$$F(q) = F(Q_0)(1 + \alpha|q|) \quad (28)$$

and with a requirement of the same slope of the intensity curves for the both signs of  $q$ .

The results are shown in Fig. 10. There are two important consequences of this approach. First, the correction led, automatically, to the same values for the left and right parts of the  $S(q)$  dependence. Second, the wings of the peaks can be fitted using a straight line in log-log plot. Both of these results confirm the necessity of the correction of the intensities by the form factor to obtain correct  $S(q)$ . Indeed, as we have discussed in Sec. III C 2, the absence of the differences in the intensities for the both signs of  $q$  means that the de Gennes's penetration depth  $\xi=(K/B)^{1/2} > 2\pi/Q_0$  [43,44], which is normally the case for the lipid membranes since their bending rigidity is quite high (about 20 kT). In addition, a good linear approximation of the wings of the diffraction peaks in log-log representation is predicted by Eq. (24).

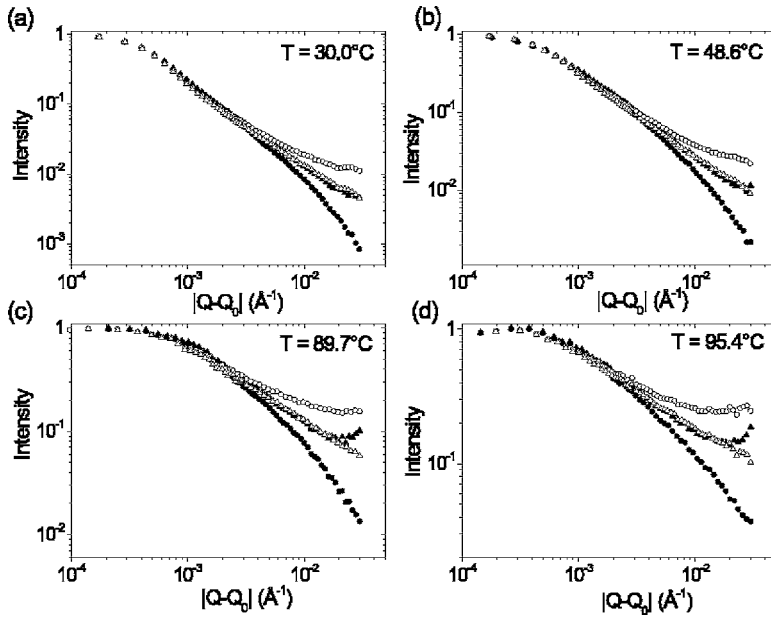


FIG. 10. Left (solid symbols) and right (empty symbols) parts of the HRXRD peak from 30% (w/w) multilamellar DMPC membranes in  $D_2O$  before (circles) and after (triangles) correction of the intensities by the form factor  $F(Q)$  at four different temperatures: (a) 30 °C, (b) 48.6 °C, (c) 89.7 °C, and (d) 95.4 °C. The correction leads to symmetric peaks with linear slope in the log-log plot as predicted by Caillé theory. To aid in visualization, data at  $|Q-Q_0| > 3 \times 10^{-3} \text{ \AA}^{-1}$  are binned, reducing number of points and distributing them equally on the logarithmic scale.

Therefore we applied the form factor corrections to diffraction peak intensities at all measured temperatures. Following this, a complete peak shape analysis was done as described in Sec. III C 2. The results of the fits at some of the temperatures are shown in Fig. 11. Dependence of the Caillé parameter  $\eta$  on temperature  $T$  is shown in Fig. 12. There are two different characteristic parts of the  $\eta(T)$  dependence: (i) slow change in the temperature interval from 48.6 to 76.8 °C and (ii) dramatic increase at  $T > 77$  °C. A comparison of Figs. 7 and 12 shows that a considerable increase in the intermembrane distance as well as in the parameter of the strength of the undulations  $\eta$  starts at the same temperature,  $\sim 77$  °C.

The mean square fluctuations of the water spacing  $\sigma_{dw}$  in multilamellar membranes are described by the following equation [83]:

$$\sigma_{dw}^2 = \beta^{-1} \eta d^2, \quad (29)$$

where  $\beta$  is a numerical parameter  $\sim 10$  [83]. The average amplitude of undulations exhibits a dramatic increase at the

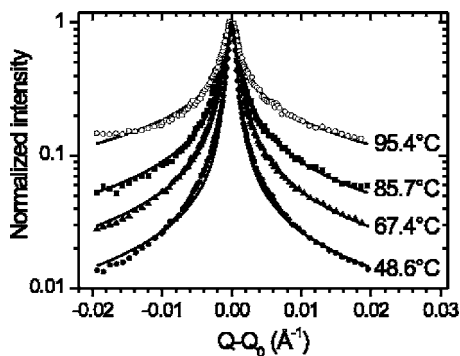


FIG. 11. Examples of the fits of the HRXRD peaks from 30% (w/w) multilamellar DMPC membranes in  $D_2O$  at different temperatures using modified Caillé theory. Peak wings are fitted very well in the wide region of  $Q$ .

temperatures higher than 77 °C, since both of the parameters  $\eta$  and  $d$  increase with temperature. It gives additional evidence of the main role of undulations in the membrane unbinding.

### C. Determination of the fundamental undulation constant

So far we have shown that the undulation force is the dominating repulsive force between freely suspended in water DMPC membranes at temperatures above 48 °C. Increasing the temperature results in the so-called unbinding transition that starts at 77 °C. The next important question is, what is the actual functional form of the undulation force? In other words, does the hard confinement Helfrich's model correctly describe dependence of the undulation force on the intermembrane distance [Eq. (4)] or should more complex models be considered? For this purpose we will use an equation derived in Ref. [83] where the undulation force is expressed through experimentally measured parameter  $\eta$  and multilamellar repeat distance  $d$ :

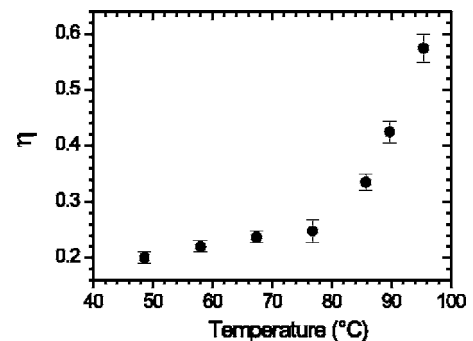


FIG. 12. Temperature dependence of the Caillé parameter  $\eta$  of undulating DMPC membranes determined from the shape analysis of the diffraction peaks.

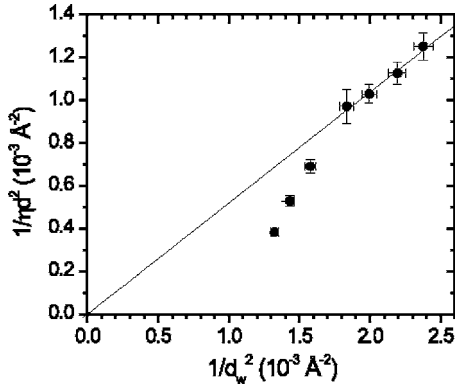


FIG. 13. The functional plot of  $1/d^2\eta$  vs  $1/d_w^2$  for DMPC membranes in  $D_2O$ . The dependence is linear in the temperature interval from 48.5 to 76.8 °C confirming applicability of the hard-wall confinement functional form [Eq. (4)] in this temperature range.

$$f_{und} = \frac{1}{4} \frac{(k_B T)^2}{k \eta d^2}. \quad (30)$$

If we assume that Eq. (4) is correct functional form of  $f_{und}$  then a plot of  $1/d^2\eta$  vs  $1/d_w^2$  should represent a straight line. Indeed, as shown in Fig. 13 the dependence is linear in the temperature interval from 48.5 to 76.8 °C proving the validity of the hard confinement functional form of Eq. (4) at these temperatures. At higher temperatures (i.e., at those temperatures at which unbinding takes place) the plot strongly deviates from the straight-line approximation confirming the anomalous behavior of the free energy in this case.

Since the hard-confinement regime is confirmed in our experimental case, we can fit the measured data to obtain the value of the fundamental constant  $c_{fl}$ . To do this we combine Eqs. (4) and (30) and rewrite them in the following form:

$$\eta = \frac{\pi}{2\sqrt{6}c_{fl}} \left(1 - \frac{d_b}{d}\right)^2. \quad (31)$$

Dependence of  $\eta$  on  $(1-d_b/d)^2$  is shown in Fig. 14 and it

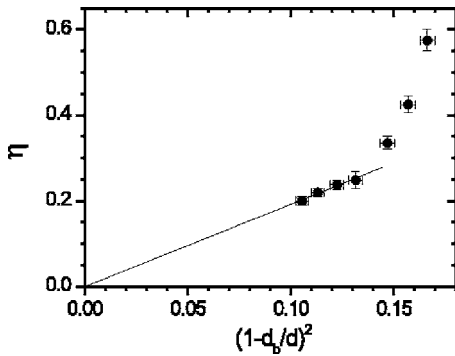


FIG. 14. Dependence of the Caillé parameter  $\eta$  on  $(1-d_b/d)^2$  for multilamellar DMPC membranes in  $D_2O$ . The linear fit is done for the data in the temperature interval from 48.5 to 76.8 °C. The slope of the line allows us to calculate value of the universal constant of the undulation force  $c_{fl}=0.111\pm 0.005$ , according to Eq. (31).

displays a linear behavior in the temperature interval from 48.6 to 76.8 °C as it was expected. At higher temperatures (i.e., at those temperatures at which unbinding takes place), the plot strongly deviates from the straight-line approximation confirming once again a qualitatively different behavior of the system at these temperatures. The linear fit of the data corresponding to the temperature interval from 48.6 to 76.8 °C is shown in Fig. 14. This fit gives the universal constant of undulation force  $c_{fl}=0.111\pm 0.005$ , which is in good agreement with all theoretical predictions [33–38,40] and is identical to  $c_{fl}=0.106$  [36] and to the most recent calculations:  $c_{fl}=0.115\pm 0.005$  [40],  $c_{fl}=0.111\pm 0.006$  [37],  $c_{fl}=0.113\pm 0.005$  [41].

It is well known that in the hard-wall confinement case the square of the mean fluctuations is proportional to the square of the interplane distance [4]:

$$\sigma_{d_w}^2 = \mu d_w^2, \quad (32)$$

where  $\mu$  is a numerical constant.

Comparing Eqs. (29) and (32) we obtain

$$\eta d^2 = \beta \mu d_w^2. \quad (33)$$

Then substituting the left part of Eq. (33) in Eq. (30) we finally get

$$f_{und} = \frac{1}{4\beta\mu} \frac{(k_B T)^2}{k d_w^2}. \quad (34)$$

Taking into account that the numerical factor in Eq. (34) must be equal to  $c_{fl}$  we can calculate  $\mu$  as

$$\mu = \frac{1}{4\beta c_{fl}}. \quad (35)$$

Assuming that  $\beta=10$  and substituting the experimental value of  $c_{fl}$  into Eq. (35) we find that  $\mu=0.225$ . This value is in agreement with theoretical result  $\mu\approx 0.2$  [40]. It is also very close to the calculated values of  $\mu=0.25$  [34] and  $\mu\approx 0.183$  [87].

To our knowledge there is only one cycle of works [42–44] where  $c_{fl}$  was experimentally measured using a similar system of fluctuated lipid membranes. The authors in Ref. [44] used a similar approach of analysis of high-resolution diffraction peaks but instead of changing temperature as in our work they added pentanol to the lipid membranes, which softened them and increased undulations and separation between membranes. The results of Refs. [42–44] were consistent with the initial estimations of the value of  $c_{fl}$  by Helfrich [4],  $c_{fl}=0.23$ , in strong disagreement with recent theoretical calculations as well as with our experimental value of  $c_{fl}=0.111\pm 0.005$ . To explain this discrepancy we would like to point out importance of the following factors for an accurate estimation of the value of the  $c_{fl}$  constant: First of all, as we have shown earlier, the intensities of the diffraction peaks should be corrected by the form factor when necessary before performing peak shape analysis. This is important for accurate determination of the Caillé parameter  $\eta$ . Second, the steric thickness of the bilayer must be

accurately determined. The importance of these corrections follows from Eq. (31). Indeed, Eq. (31) can be rewritten in the form

$$\eta = \frac{\pi}{2\sqrt{6}c_{fl}} \left( \frac{d_w}{d} \right)^2, \quad (36)$$

from which the following equations can be derived:

$$\frac{\Delta c_{fl}}{c_{fl}} = 4 \frac{\Delta d_w}{d_w} \quad \text{and} \quad \frac{\Delta c_{fl}}{c_{fl}} = -2 \frac{\Delta \eta}{\eta}. \quad (37)$$

Equation (37) shows that the error in the determination of  $c_{fl}$  is strongly affected by the error of  $\eta$  and dramatically by the error of  $d_w$ . In Ref. [44] Luzzati approach [88] was applied to obtain  $d_w$  from a measured repeat distance and known fraction of water in the sample. This approach assumes no water penetration into lipid bilayer and tends to underestimate the actual steric bilayer thickness by at least

$$\Delta d_w = 2V_w/A_L, \quad (38)$$

where  $V_w$  is the volume of water in the lipid bilayer and  $A_L$  is the area per lipid molecule. Substituting  $V_w = 7.2 \times 30 \text{ \AA}^3$  and  $A_L = 59.6 \text{ \AA}^2$  for DMPC membranes in excess water at 30 °C [70] into Eq. (38) we get  $\Delta d_w = 7.2 \text{ \AA}$ . This could result in considerable overestimation of the value of intermembrane distances. It is true that this effect becomes less important at large intermembrane spacings as in Refs. [42–44]. However, we took experimental data from Ref. [44] measured at largest separation between membranes (20% H<sub>2</sub>O by volume,  $d = 157 \text{ \AA}$ , and  $\eta = 1$ ) and estimated value of the  $c_{fl}$  using the Luzzati approximation, corrected as described above. We obtained  $c_{fl} = 0.144$ , which is closer to the value obtained in this work, 0.111, than to the initial Helfrich’s estimation, 0.23. In addition, using highly swollen membranes has its own caveat that the intensities of the diffraction peaks become rather weak and therefore accuracy of the peak shape analysis used for determination of the parameter  $\eta$  is not high at these spacings [42–44]. It can be an additional source of error in the evaluation of the value of the  $c_{fl}$  constant. Thus this exercise demonstrates the significance of the possible errors in determination of the Caillé parameter  $\eta$  and especially of the bilayer thickness on the reliability of obtained values of the universal constant  $c_{fl}$ .

## V. CONCLUSIONS

We performed a comprehensive study of temperature dependence of the intermembrane force balance for multilamellar DMPC membranes freely suspended in D<sub>2</sub>O. The emphasis was on the accurate determination of the intermembrane distance in a wide range of temperatures from ~40 to 110 °C using SANS from unilamellar and multilamellar membranes and on obtaining accurate values of the Caillé parameter  $\eta$  from HRXRD experiments at the same temperatures.

The experiments revealed a dominating role of Helfrich’s undulation force in the whole measured temperature interval. At ~77 °C the onset of the unbinding transition in the multilamellar membranes is observed. The transition has a con-

tinuous character as was predicted by the theoretical model used by Lipowsky and Leibler [45]. SANS data suggest that the unbinding transition proceeds in accordance with the two-state model [50].

Complementary analysis of the SANS and HRXRD data allows us to estimate the value of the undulation force universal constant  $c_{fl} = 0.111 \pm 0.005$ . This value is approximately two times smaller than the initial estimate, 0.23, done by Helfrich [4] and early experimental values [42–44], that confirmed Helfrich’s estimation, but is in good agreement with more recent theoretical simulations and analytical calculations of the constant  $c_{fl} = 0.106$  [36],  $0.115 \pm 0.005$  [40],  $0.111 \pm 0.006$  [37], and  $0.113 \pm 0.005$  [41].

## ACKNOWLEDGMENTS

We thank G. Bueldt for his generous support of this project. We acknowledge T. Zemb and J. Lambard for providing time and help during x-ray high-resolution test experiments at their Bose-Harte camera, O. Diat for his assistance during experiments at the ESRF, G. Gompper and Y. Miskuita for careful reading of the manuscript. V.I.G. is grateful to Alexander von Humboldt Foundation for the support of the project.

## APPENDIX A: PEAK SHAPE ANALYSIS

In a general case the scattering intensity from a stack of membranes is described by

$$S(\mathbf{Q}) \propto \int_{-\infty}^{+\infty} d^3R H(\mathbf{R}) G(\mathbf{R}) e^{i(\mathbf{Q}-n\mathbf{Q}_0) \cdot \mathbf{R}}, \quad (A1)$$

where  $H(\mathbf{R})$  is the function, that describes the finite-size effect, due to the finite thickness of a multilayer sample.

In the case of the centrosymmetric lipid membrane Eq. (A1) is rewritten in the following form [81]:

$$S(Q) = 2\pi \int_{-\infty}^{\infty} \int_{-\infty}^{\infty} dz P(r, z) G(r, z) \cos(Q_0 z) \frac{\sin Q \sqrt{r^2 + z^2}}{Q \sqrt{r^2 + z^2}}. \quad (A2)$$

If the asymmetry of the diffraction peak is not observable, then Eq. (A2) is modified to [81]

$$S(Q) = \frac{2\pi L_0^2 \int_0^{\infty} dLP(L) \int_0^L dz G_A(0, z) (L-z) \cos(Q-Q_0)z}{\int_0^{\infty} dLP(L)}, \quad (A3)$$

where

$$G_A(0, z) = \exp\left(-\eta \sum_{n=0}^N \frac{1 - \cos(n-z)/L}{n}\right). \quad (A4)$$

Equation (A3) is Eq. (80) from Ref. [81]. Gaussian distribution of the domain sizes,

$$P(L) \propto e^{-(L-L_0)^2/2\sigma_L^2}, \quad (\text{A5})$$

was used in Eq. (A3).

**APPENDIX B: CORRECTION OF THE MEMBRANE THICKNESS FOR TEMPERATURE DEPENDENCE OF THE AMOUNT OF WATER IN THE POLAR PART OF THE MEMBRANES**

Taking into account dependence of  $V_w/V_L$  on temperature leads to the following modification of Eq. (15):

$$\begin{aligned} d_b'^T &= d_b' \left[ 1 - 1.26 \frac{V_w}{V_L} - 1.26 \Delta \left( \frac{V_w}{V_L} \right) \right]^{-1/2} \\ &= d_b' \left( 1 - \frac{1.26 \Delta \left( \frac{V_w}{V_L} \right)}{1 - 1.26 \frac{V_w}{V_L}} \right)^{-1/2} \\ &= d_b' \left( 1 - \frac{1.26 \left( \Delta V_w - \frac{\Delta V_L}{V_L} V_w \right)}{V_L \left( 1 - 1.26 \frac{V_w}{V_L} \right)} \right)^{-1/2}. \end{aligned} \quad (\text{B1})$$

The increase of the water content in the bilayer  $\Delta V_w$  with

temperature can be calculated using the following equation:

$$\Delta V_w = \frac{d_b' A_L}{2} \left( \frac{\Delta d_b'}{d_b'} + \frac{\Delta A_L}{A_L} \right) - \frac{\Delta V_L}{V_L} V_L, \quad (\text{B2})$$

where  $A_L = 59.6 \text{ \AA}^2$  is the area per DMPC lipid molecule [70];  $\Delta d_b'/d_b'$  is obtained experimentally in this work (see Fig. 4); the thermal expansivities of the volume and area per DMPC molecule were taken from literature:  $(1/A_L) \times (\Delta A_L/\Delta T) = 3.3 \times 10^{-3} \text{ K}^{-1}$  [70,89],  $(1/V_L)(\Delta V_L/\Delta T) = 0.5 \times 10^{-3} \text{ K}^{-1}$  [74,90]. Substituting  $\Delta V_w$  from Eq. (B2) into Eq. (B1) and the value of the corresponding parameters gives the following equation:

$$\begin{aligned} d_b'^T &= d_b' [1 - 15.4 \times 10^{-4} (T - 30)]^{-1/2} \\ &\approx d_b' [1 + 7.7 \times 10^{-4} (T - 30)], \end{aligned} \quad (\text{B3})$$

where  $T$  is the temperature in  $^\circ\text{C}$ . Equations (13), (15), and (B3) were used to determine the thickness of DMPC bilayer at different temperatures.

- 
- [1] R. B. Gennis, *Biomembranes* (Springer-Verlag, New York, 1989).
- [2] G. Ceve and D. Marsh, *Phospholipid Bilayers* (John Wiley, New York, 1987).
- [3] Y. Namba, in *Phospholipid Handbook*, edited by G. Ceve (Marcel Dekker, Inc., New York, 1993).
- [4] W. Helfrich, *Z. Naturforsch. A* **33A**, 305 (1978).
- [5] *Proceedings of Jerusalem Winter School of Theoretical Physics, 1987/88*, edited by D. R. Nelson, T. Pizan, and S. Weinberg (World Scientific, Singapore, 1989), Vol. 5.
- [6] R. Lipowsky, *Nature (London)* **349**, 475 (1991).
- [7] A. Polyakov, *Nucl. Phys. B* **268**, 406 (1986).
- [8] H. Kleinert, *Phys. Lett. B* **174**, 335 (1986).
- [9] W. Janke, *Int. J. Mod. Phys. B* **4**, 1763 (1990).
- [10] J. Israelachvili and H. Wennerström, *Nature (London)* **379**, 219 (1996).
- [11] R. P. Rand and A. Parsegian, *Biochim. Biophys. Acta* **288**, 351 (1989).
- [12] S. Leikin, V. A. Parsegian, and D. C. Rau, *Annu. Rev. Phys. Chem.* **44**, 369 (1993).
- [13] J. Israelachvili and H. Wennerström, *Langmuir* **6**, 873 (1990).
- [14] J. Israelachvili and H. Wennerström, *J. Phys. Chem.* **96**, 520 (1999).
- [15] T. J. McIntosh and S. A. Simon, *Annu. Rev. Biophys. Biomol. Struct.* **23**, 27 (1994).
- [16] V. I. Gordeliy, V. G. Cherezov, A. V. Anikin, M. V. Anikin, V. V. Chupin, and J. Teixeira, *Prog. Colloid Polym. Sci.* **100**, 338 (1996).
- [17] V. I. Gordeliy, V. G. Cherezov, and J. Teixeira, *J. Mol. Struct.* **383**, 117 (1996).
- [18] V. I. Gordeliy, *Langmuir* **12**, 3498 (1996).
- [19] R. Aveyard and D. A. Haydon, *Trans. Faraday Soc.* **61**, 2255 (1965).
- [20] R. Lipowsky and S. Grothans, *Europhys. Lett.* **23**, 599 (1993).
- [21] R. Lipowsky and S. Grothans, *Biophys. Chem.* **49**, 27 (1994).
- [22] *Structure and Dynamics of the Membranes*, edited by R. Lipowsky and E. Sackmann (Elsevier, Amsterdam-Tokyo, 1995), Vol. 2.
- [23] J. N. Israelachvili, *Intermolecular and Surface Forces* (Academic Press, New York, 1991).
- [24] J. Marra and J. N. Israelachvili, *Biochemistry* **24**, 4608 (1985).
- [25] J. Marra, *J. Colloid Interface Sci.* **109**, 10 (1986).
- [26] L. Fernandez-Puente, I. Bivas, M. D. Mitov, and P. Mélléard, *Europhys. Lett.* **28**, 181 (1994).
- [27] H. Engelhardt, H. P. Duwe, and E. Sackmann, *J. Phys. (Paris), Lett.* **46**, 395 (1985).
- [28] H. P. Duwe, J. Käs, and E. Sackmann, *J. Phys. (Paris)* **51**, 945 (1990).
- [29] E. Evans and W. Rawicz, *Phys. Rev. Lett.* **64**, 2094 (1990).
- [30] D. C. Wack and W. W. Webb, *Phys. Rev. A* **40**, 1627 (1989).
- [31] W. Janke and H. Kleinert, *Phys. Rev. Lett.* **58**, 144 (1987).
- [32] H. Kleinert, *Phys. Lett. A* **138**, 201 (1989).
- [33] F. David, *J. Phys. (Paris), Colloq.* **51**, C7-115 (1990).
- [34] W. Janke and H. Kleinert, *Phys. Lett. A* **117**, 353 (1986).
- [35] W. Janke, H. Kleinert, and M. Meinhardt, *Phys. Lett. B* **217**, 525 (1989).

- [36] G. Gompper and D. M. Kroll, *Europhys. Lett.* **9**, 59 (1989).
- [37] R. R. Netz and R. Lipowsky, *Europhys. Lett.* **29**, 345 (1995).
- [38] R. R. Netz, *Phys. Rev. E* **51**, 2286 (1995).
- [39] H. Kleinert, *Phys. Lett. A* **257**, 269 (1999).
- [40] R. Lipowsky and B. Zielinska, *Phys. Rev. Lett.* **62**, 1572 (1989).
- [41] R. Netz, Ph.D. thesis, University of Cologne, Cologne, 1994.
- [42] C. R. Safinya, D. Roux, G. S. Smith, S. K. Sinha, P. Dimon, N. A. Clark, and A. M. Bellocq, *Phys. Rev. Lett.* **57**, 2718 (1986).
- [43] D. Roux and C. R. Safinya, *J. Phys. (Paris)* **49**, 307 (1988).
- [44] C. R. Safinya, E. B. Sirota, D. Roux, and G. S. Smith, *Phys. Rev. Lett.* **62**, 1134 (1989).
- [45] R. Lipowsky and S. Leibler, *Phys. Rev. Lett.* **56**, 2541 (1986).
- [46] H. Wennerström, *Langmuir* **6**, 834 (1990).
- [47] R. Lipowsky, *Phys. Scr., T* **29**, 259 (1989).
- [48] R. Lipowsky and M. E. Fisher, *Phys. Rev. B* **36**, 2126 (1987).
- [49] R. Lipowsky, Ph.D. thesis, University of Munich, Munich, 1987.
- [50] R. Lipowsky, in *Structure and Dynamics of Membranes* (Elsevier, Amsterdam, 1995).
- [51] T. W. Burkhardt and P. Schlottmann, *J. Phys. A* **26**, L501 (1993).
- [52] W. Helfrich, *J. Phys. II* **3**, 385 (1993).
- [53] S. T. Milner and D. Roux, *J. Phys. II* **2**, 1741 (1992).
- [54] R. R. Netz and R. Lipowsky, *Phys. Rev. Lett.* **71**, 3596 (1993).
- [55] R. M. Servuss and W. Helfrich, *Biochim. Biophys. Acta* **436**, 900 (1976).
- [56] W. Harbich, R. M. Servuss, and W. Helfrich, *Phys. Lett.* **57A**, 294 (1976).
- [57] R. M. Servuss and W. Helfrich, *J. Phys. (Paris)* **50**, 809 (1989).
- [58] W. Helfrich, *J. Phys. (Paris)* **51**, 1027 (1990).
- [59] W. Helfrich, in *Structure and Dynamics of Membranes* (Elsevier, Amsterdam, 1995).
- [60] E. Evans and M. Metcalfe, *Biophys. J.* **46**, 423 (1984).
- [61] E. Evans and D. Needham, *J. Phys. Chem.* **91**, 4219 (1987).
- [62] M. Mutz and W. Helfrich, *Phys. Rev. Lett.* **62**, 2881 (1989).
- [63] M. Vogel, C. Munster, W. Fenzl, and T. Salditt, *Phys. Rev. Lett.* **84**, 390 (2000).
- [64] R. Podgornik and V. A. Parsegian, *Biophys. J.* **72**, 942 (1997).
- [65] S. Kirchner and G. Ceve, *Europhys. Lett.* **23**, 229 (1993).
- [66] R. C. MacDonald, R. I. MacDonald, B. Ph. M. Menco, K. Takeshita, N. K. Subarao, and Hu Lang-rong, *Biochim. Biophys. Acta* **1061**, 297 (1991).
- [67] V. I. Gordeliy, L. V. Golubchikova, A. Kuklin, A. G. Syrykh, and A. Watts, *Colloid Polym. Sci.* **93**, 38 (1993).
- [68] L. A. Feigin and D. I. Svergun, *Structure Analysis by Small-angle X-ray and Neutron Scattering* (Plenum Press, New York and London, 1987).
- [69] D. M. Sadler, F. Reiss-Husson, and E. Rivas, *Chem. Phys. Lipids* **52**, 41 (1990).
- [70] J. Nagle and S. Tristram-Nagle, *Biochim. Biophys. Acta* **1469**, 159 (2000).
- [71] V. I. Gordeliy, Ph.D. thesis, Joint Institute for Nuclear Research, Dubna, 1989.
- [72] I. A. Vasilenko, V. I. Gordeliy, L. A. Tonkonog, and V. L. Borovyagin, *Biol. Membr.* **5**, 428 (1988).
- [73] S.-W. Chiy, M. Clark, V. Balaji, S. Subramaniam, H. L. Scott, and E. Jakobsson, *Biophys. J.* **69**, 1230 (1995).
- [74] H. I. Petrache, S. Tristram-Nagle, and J. F. Nagle, *Chem. Phys. Lipids* **95**, 83 (1998).
- [75] J. F. Nagle and D. A. Wilkinson, *Biophys. J.* **23**, 159 (1978).
- [76] C. Rieckel, P. Bosecke, O. Diat, and P. Engstrom, *J. Mol. Struct.* **383**, 291 (1996).
- [77] A. Caillé, *C. R. Seances Acad. Sci., Ser. B* **274**, 891 (1972).
- [78] L. D. Landau, in *Collected Papers of L.D. Landau*, edited by D. Haar (Gordon and Breach, New York, 1965), p. 245.
- [79] R. E. Peierls, *Helv. Chir. Acta Suppl.* **7**, 81 (1934).
- [80] J. Als-Nielsen, J. D. Litster, R. J. Birgeneau, M. Kaplan, C. R. Safinya, A. Lindegaard-Andersen, and S. Mathiesen, *Phys. Rev. B* **22**, 312 (1980).
- [81] R. Zhang, S. Tristram-Nagle, W. Sun, R. L. Headrick, T. C. Irving, R. M. Suter, and J. F. Nagle, *Biophys. J.* **70**, 349 (1996).
- [82] R. Zhang, W. Sun, S. Tristram-Nagle, R. L. Headrick, R. M. Suter, and J. F. Nagle, *Phys. Rev. Lett.* **74**, 2832 (1995).
- [83] H. I. Petrache, N. Gouliarov, S. Tristram-Nagle, R. Zhang, R. M. Suter, and J. F. Nagle, *Phys. Rev. E* **57**, 7014 (1998).
- [84] V. M. Kaganer, B. I. Ostrovskii, and W. H. de Jeu, *Phys. Rev. A* **44**, 8158 (1991).
- [85] F. James, CERN program library long writeup D506 (1998).
- [86] P. Balgavý, D. Uhríkova, V. I. Gordeliy, and V. G. Cherezov, *Acta Phys. Slov.* **51**, 53 (2001).
- [87] R. Podgornik and V. A. Parsegian, *Langmuir* **8**, 557 (1992).
- [88] V. Luzzati and F. Husson, *J. Cell Biol.* **12**, 207 (1962).
- [89] E. A. Evans and D. Needham, *J. Phys. Chem.* **91**, 4219 (1987).
- [90] M. C. Wiener, S. Tristram-Nagle, D. A. Wilkinson, L. E. Campbell, and J. F. Nagle, *Biochim. Biophys. Acta* **938**, 135 (2004).
- [91] N. Kucerka, M. Kiselev, and P. Balgavy, *Eur. Biophys. J.* **33**, 328 (2004).